Available online at www.sciencedirect.com
ScienceDirect
C. R. Mecanique 337 (2009) 303–311
COMPTES RENDUS MECANIQUE

Analytical modeling of rail vehicle safety and comfort in short radius curved tracks

Mohamed Nejlaoui [a], Zouhaier Affi [a,*], Ajmi Houidi [b], Lotfi Romdhane [c]

[a] *Laboratoire de génie mécanique, École nationale d'ingénieurs de Monastir, avenue Ibn-Eljazzar, 5019 Monastir, Tunisia*
[b] *Laboratoire de génie mécanique, institut supérieur des sciences appliquées de Sousse, Sousse, Tunisia Cité Etaffela, 4003 Sousse Ibn khouldoun, Tunisia*
[c] *Laboratoire de génie mécanique, École nationale d'ingénieurs de Sousse, avenue 18 janvier, Bab jedid, 4000 Sousse, Tunisia*

Received 2 January 2009; accepted after revision 28 May 2009

Available online 23 June 2009

Presented by Jean-Baptiste Leblond

Abstract

This study deals with the modeling of rail vehicles' behavior when traveling in curves of short radius. Based on the symmetry of the vehicle and on the nature of the motion, we show that the study of the system behavior can be reduced to the quasi static study of a quarter. We propose in this work, an analytical model able to describe the safety and the comfort by determining derailment and creep forces. The developed model is validated using the software ADAMS and results from the bibliography. The developed model can be easily used to optimize the rail vehicles design and the sensitivity analyses of its performance. ***To cite this article: M. Nejlaoui et al., C. R. Mecanique 337 (2009).***

Keywords: Modeling; Rail vehicles; Short radius curves; Safety; Comfort

1. Introduction

Safety and comfort are two imperative criteria for traveling rail vehicles. Traveling on curves of short radius, the rail vehicle (RV) can circulate with creep wheel–rail (WR) causing wear and noise. Moreover, the RV circulates, in general, with contact flange–rail which can create a derailment. There are several works dealing with these problems.

Dang Van [1] has presented the fatigue damage prediction methodology applicable to multiaxial fatigue conditions of the wheel–rail system. Joly [2] has presented the WR contact forces in closed form. Shevtsov et al. [3] have defined a design procedure for a wheel profile based on geometrical WR contact characteristics. They checked the optimized results with ADAMS software.

Majka et al. [4] have studied the effects of some design parameters on the dynamic response of railway bridges. Vehicle damping was found to have an negligible influence on the system dynamic response. He and McPhee [5]

* Corresponding author.
E-mail addresses: zouhaier.affi@enim.rnu.tn (Z. Affi), ajmi.houidi@issatso.rnu.tn (A. Houidi), lotfi.romdhane@enim.rnu.tn (L. Romdhane).

1631-0721/$ – see front matter
doi:10.1016/j.crme.2009.05.003

Nomenclature

i	index of wheel set	y_k	transversal displacement of the bogie k
j	index of wheel	$\bar{y}$	transversal displacement of the car body
k	index of bogie	α_{ki}	yaw angle of the wheelset i of the bogie k
g	the gravity constant	α_k	yaw angle of the bogie k
G_{ki}	wheelset centre of mass	$\bar{\alpha}$	yaw angle the car body
G_k	bogie centre of mass	ς_u	gyration radius of the wheelset around the direction u ($u = x, y, z$)
$\bar{G}$	car body centre of mass		
m	wheelset mass	Ω_u	gyration radius of the bogies around the direction u
$\hat{m}$	bearing box body mass		
M	mass of bogie	$\bar{\Omega}_u$	gyration radius of the car body around the direction u
$\bar{M}$	car body mass		
N	normal load by a wheel	K_u	spring stiffness of the primary suspension in the direction u
R_c	radius of curve		
y_{ki}	transversal displacement of the wheelset i of bogie k	$\bar{K}_u$	spring stiffness of the secondary suspension in the direction u

have used multibody dynamic modeling software to determine the governing equations of motion of the RV models. Based on this model, a design optimization was conducted. Rjeb et al. [6] have optimized the design variables of RV system in rectilinear motion using Genetic Algorithms. Elkins and Wu [7] considered the ratio of the lateral force to the vertical force applied by each wheel as a derailment criterion.

It seems that no literature has reported the performance such as safety and comfort of the RV system in closed form. The main factor that hinders this approach is the great complexity of the system. The goal of this work is the modeling of the RV behavior in short radius curves in closed form. In Section 2, we describe the RV structure. Section 3 reports the dynamic modeling of the system. In Section 4, we quantify the comfort and safety criterion in terms of contact forces. The validation of the proposed model is presented in Section 5. Some concluding remarks are given in Section 6.

2. The rail vehicle structure

The RV is made of a car body, two bogies and four wheelsets. The car body C is connected to the bogies C_k by 4 secondary suspensions. Each bogie is connected to 2 wheelsets S_{ki} using 4 primary suspensions. In the real design, each suspension is formed by a vertical spring and a damper in parallel. Each one works in the 3 directions with different stiffness and damping coefficients [2]. Generally, each suspension is modeled by 3 systems, formed by springs and dampers in parallel (Fig. 1), acting in the 3 directions (i.e. longitudinal (1), lateral (2) and vertical (3)) [2,5,10,11].

In order to model the dynamic behavior of the rail vehicle, different reference frames were used. A fixed reference frame $R_g = (O_g, X_g, Y_g, Z_g)$ is attached to the track. To each body forming the system we have a reference frame $R_i = (G_i, X_i, Y_i, Z_i)$. $R_0 = (O_0, X_0, Y_0, Z_0)$ is an inertial reference frame attached to the rail vehicle. The RV system has 21 degrees of freedom, which are summarized in Table 1.

The RV system has a longitudinal symmetry. This symmetry leads to the decoupling of lateral, vertical and longitudinal motions [2]. In this Note we focus on the lateral dynamic of the RV system. In order to simplify the modeling of the RV system and without loss of generality, we will consider only one quarter (Fig. 1). The quarter of the RV has 8 degrees of freedom, with respect to the frame $R_0 = (O_0, X_0, Y_0, Z_0)$. These motions are represented by the generalized coordinate vector $\mathbf{q}$.

$$\mathbf{q} = [\bar{y}, \bar{\alpha}, y_1, \alpha_1, y_{11}, \alpha_{11}, y_{12}, \alpha_{12}]^T \tag{1}$$

In this study, we assume that the rail curve radius and the rail inclination, δ, are constant. Moreover, in curves, the RV has a constant and a low traveling speed. Consequently, the roll motion and the damping forces are not significant compared to the elastic forces.

Table 1
Degrees of freedom of the RV system.

	Lateral displacement	The roll	The yaw
Car body	$\bar{y}$	$\bar{\theta}$	$\bar{\alpha}$
Bogies C_k $(k = 1, 2)$	y_k	θ_k	α_k
Wheelsets S_{ki} $(k, i = 1, 2)$	y_{ki}	θ_{ki}	α_{ki}

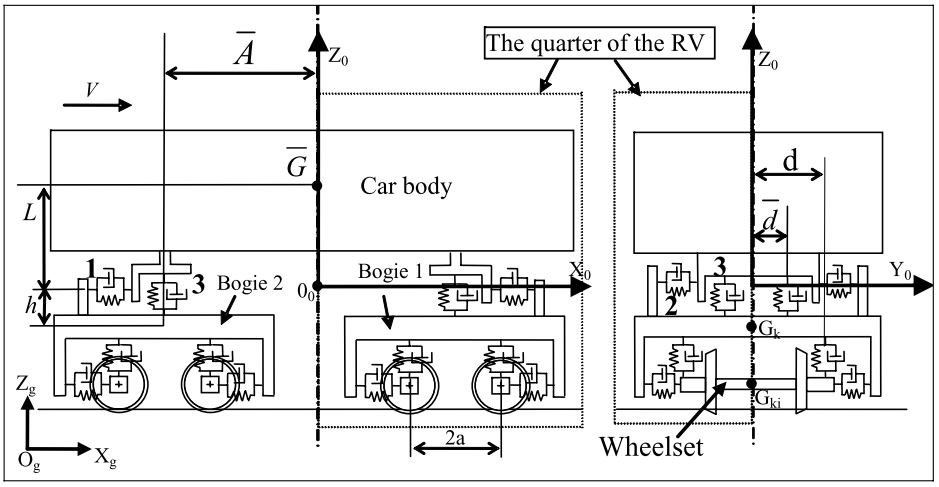

Fig. 1. The rail vehicle model.

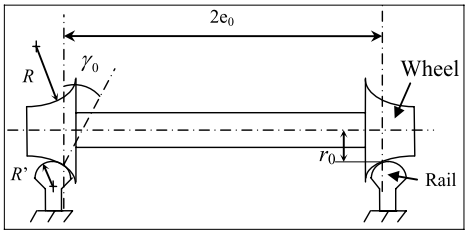

Fig. 2. The geometric parameters of the WR.

3. The dynamic modeling of rail vehicle

3.1. Kinematics study of the rail vehicle

In curved track, the wheelset has a lateral displacement, y_0, which leads to a pure rolling configuration. We consider the expression of the wheelset lateral displacement y_0 given by [2]:

$$y_0 = \frac{e_0 r_0}{\gamma_e R_c} \tag{2}$$

with

$$\gamma_e = \frac{R\gamma_0}{R - R'} \frac{e_0 + R'\gamma_0}{e_0 - r_0\gamma_0}$$

The geometric parameters e_0, r_0, γ_0, R and R' are described in Fig. 2.

By considering the lateral displacement of the wheel set, the quarter RV generalized coordinates in a curved track will be:

$$y_{11}^* = y_{11} + y_0, \quad y_{12}^* = y_{12} + y_0, \quad y_1^* = y_1 + \frac{y_{11} + y_{12}}{2} + y_0, \quad \alpha_1^* = \alpha_1 + \frac{y_{11} - y_{12}}{2a} \quad \text{and}$$

$$\bar{y}^* = \bar{y} + y_1 + \frac{y_{11} + y_{12}}{2} + y_0 \tag{3}$$

Due to the RV symmetries, the bogies have the same, but opposite, magnitude of lateral displacements. Consequently, the car body yaw angle can be written as:

$$\bar{\alpha}^* = \bar{\alpha} + \frac{y_1 - y_2}{2\bar{A}} = \bar{\alpha} + \frac{y_1}{\bar{A}} \tag{4}$$

Hence, the quarter RV coordinate vector will be:

$$\mathbf{q} = [\bar{Y}^*, \bar{\alpha}^*, Y_1^*, \alpha_1^*, y_{11}^*, \alpha_{11}, y_{12}^*, \alpha_{12}]_{R_0}^T \tag{5}$$

3.2. The dynamic model

The dynamic model of the RV is developed based on the Lagrange formalism given by:

$$\frac{\mathrm{d}}{\mathrm{d}t}\left(\frac{\partial L}{\partial \dot{q}_i}\right) - \frac{\partial L}{\partial q_i} = Q_i \tag{6}$$

L and Q_i are, respectively, the Lagrangian function and the generalized forces applied to the system.

The dynamic model of the RV expressed in the moving frame R_0, can be rewritten as follows:

$$\frac{\mathrm{d}}{\mathrm{d}t}\left(\frac{\partial T}{\partial \dot{q}_i}\right) - \frac{\partial T}{\partial q_i} = Q_i - \sum_{j=1}^{4} \frac{\partial}{\partial \dot{q}_i}\{\vartheta_{S_j \in R_0/R_g}\}\{T_{S_j \in R_0/R_g}\} \tag{7}$$

where $T = T(q_i, q_i', t)$ is the kinetic energy of the system written in the reference frame R_0. S_j can be the quarter of the car body or the bogie or one of the wheelsets and $\{T_{S_j}\}, \{\vartheta_{S_j}\}$ are, respectively, the dynamic screw and the twist of $(S_j \in R_0/R_g)$ [2].

The RV kinetic energy in R_0 is given by:

$$2T = \frac{\bar{M}}{4}\left(\dot{\bar{y}}^2 + \bar{\Omega}_z^2 \dot{\bar{\alpha}}^2\right) + \frac{M}{2}\left(\dot{y}_1^2 + \Omega_z^2 \dot{\alpha}_1^2\right) + \sum_{i=1}^{i=2}\left\{(m + \hat{m})\dot{y}_{1i}^2 + \left(m\varsigma_z^2 + \hat{m}d^2\right)\dot{\alpha}_{1i}^2\right\} \tag{8}$$

The RV system generalized forces are determined via the generalized power of the different mechanical actions. These actions are those due to the gravity $\mathbf{Q}_1$, to the springs $\mathbf{Q}_2$, and to the WR contacts $\mathbf{Q}_3$. The global generalized force is given by:

$$\mathbf{Q} = \mathbf{Q}_1 + \mathbf{Q}_2 + \mathbf{Q}_3 \tag{9}$$

with

$$\mathbf{Q}_1 = \begin{bmatrix} \frac{\bar{M}}{4} g\delta \\ 0 \\ \frac{M}{2} g\delta \\ 0 \\ (m + \hat{m})g\delta + W\zeta(y_{11}^* + y_0) \\ -W\gamma_0\varepsilon_0\alpha_{11} \\ (m + \hat{m})g\delta + W\zeta(y_{12}^* + y_0) \\ -W\gamma_0\varepsilon_0\alpha_{12} \end{bmatrix}^T, \quad \mathbf{Q}_2 = \begin{bmatrix} \bar{K}_y(\bar{y}^* + \bar{A}\bar{\alpha}^*) \\ 2\bar{K}_x\bar{d}^2\beta + \bar{K}_y(\bar{A}\bar{\alpha}^* + \bar{y}^*) \\ 4K_y y_1^* + \bar{K}_y(\bar{A}\bar{\alpha}^* + \bar{y}^*) \\ \begin{pmatrix} -2\bar{K}_x\bar{d}^2(\beta + \frac{\bar{A}}{R_c}) \\ +4K_y a^2\alpha_1^* + \sum_{i=1}^{i=2} 2K_x d^2\eta_i \end{pmatrix} \\ -2K_y(y_1^* + a\alpha_1^*) \\ -2K_x d^2(\eta_1 + \frac{a}{R_c}) \\ -2K_y(y_1^* - a\alpha_1^*) \\ -2K_x d^2(\eta_2 - \frac{a}{R_c}) \end{bmatrix}^T \quad \text{and}$$

$$\mathbf{Q}_3 = \begin{bmatrix} 0 \\ 0 \\ 0 \\ 0 \\ -2C_{22}\alpha_{11}\chi\Sigma_1 \\ 2C_{11}e_0\frac{\gamma_e}{r_0}y_{11}^*\sigma_1 + 2C_{23}\alpha_{11} \\ -2C_{22}\alpha_{12}\chi\Sigma_2 \\ 2C_{11}e_0\frac{\gamma_e}{r_0}y_{12}^*\sigma_2 + 2C_{23}\alpha_{12} \end{bmatrix}^T \tag{10}$$

where:

$$\sigma_i = 1 - \frac{C_{11}}{3\mu N}\frac{\gamma_e}{r_0}y_{1i}^* + \frac{C_{11}^2}{27\mu^2N^2}\left(\frac{\gamma_e}{r_0}y_{1i}^*\right)^2, \quad \sum_i = 1 - \frac{C_{22}}{3\mu N}\alpha_{1i} + \frac{C_{22}^2}{27\mu^2N^2}\alpha_{1i}^2$$

$$\zeta = \frac{1}{(R-R')}\left(\frac{e_0 + R\gamma_0}{e_0 - r_0\gamma_0}\right)^2$$

$$\varepsilon_0 = (R+2r_0)\gamma_0 - e_0, \quad \chi = \frac{e_0}{(e_0 - r_0\gamma_0)}, \quad W = \left(\frac{\bar{M}}{4} + \frac{M}{2} + m + \hat{m}\right)g$$

$$\beta = \bar{\alpha}^* + \frac{y_1^*}{\bar{A}} - \frac{y_{11}^* - y_{12}^*}{2a} - \alpha_1^* \quad \text{and} \quad \eta_i = \alpha_1^* + \frac{y_{11}^* - y_{12}^*}{2a} - \alpha_{1i} \quad (i = 1, 2)$$

The use of Eq. (7) gives us the following RV dynamic model:

$$\mathbf{A}(\mathbf{q})\mathbf{q} = \mathbf{b} \tag{11}$$

where:

$$\mathbf{A}(q) = \begin{bmatrix} \bar{K}_y & \bar{K}_y\bar{A} & 0 & 0 & 0 \\ \bar{K}_y & 2\bar{K}_x\bar{d}^2 + \bar{K}_y\bar{A} & \frac{2\bar{K}_x\bar{d}^2}{\bar{A}} & -2\bar{K}_x\bar{d}^2 & -\frac{\bar{K}_x\bar{d}^2}{a} \\ \bar{K}_y & \bar{K}_y\bar{A} & 4K_y & 0 & 0 \\ 0 & -2\bar{K}_x\bar{d}^2 & \frac{-2\bar{K}_x\bar{d}^2}{\bar{A}} & 2\bar{K}_x\bar{d}^2 + 4K_xd^2 + 4K_ya^2 & \bar{K}_x\frac{\bar{d}^2}{a} + 2K_x\frac{d^2}{a} \\ 0 & 0 & -2Ky & -2K_ya & W\zeta \\ 0 & 0 & 0 & -2K_xd^2 & -K_x\frac{d^2}{a} + 2e_0C_{11}\frac{\gamma_e}{r_0}\sigma_1 \\ 0 & 0 & -2Ky & 2K_ya & 0 \\ 0 & 0 & 0 & -2K_xd^2 & \frac{-K_xd^2}{a} \end{bmatrix}$$

$$\begin{bmatrix} 0 & 0 & 0 \\ 0 & \frac{\bar{K}_x\bar{d}^2}{a} & 0 \\ 0 & 0 & 0 \\ -2K_xd^2 & -\bar{K}_x\frac{\bar{d}^2}{a} - 2K_x\frac{d^2}{a} & -2K_xd^2 \\ -2\chi C_{22}\sum_1 & 0 & 0 \\ 2K_xd^2 - W\gamma_0\varepsilon_0 + 2C_{23} & \frac{K_xd^2}{a} & 0 \\ 0 & W\zeta & -2\chi C_{22}\sum_2 \\ 0 & K_x\frac{d^2}{a} + 2e_0C_{11}\frac{\gamma_e}{r_0}\sigma_2 & 2K_xd^2 - W\gamma_0\varepsilon_0 + 2C_{23} \end{bmatrix}$$

$$\mathbf{b} = \left[\ \tfrac{\bar{M}}{4}\gamma_{nc} \quad 0 \quad \tfrac{M}{2}\gamma_{nc} \quad 2\bar{K}_x\bar{d}^2\tfrac{\bar{A}}{R_c} \quad (m+\hat{m})\gamma_{nc} - W\zeta y_0 \quad 2K_xd^2\tfrac{a}{R_c} \quad (m+\hat{m})\gamma_{nc} - W\zeta y_0 \quad -2K_xd^2\tfrac{a}{R_c}\ \right]^T$$

$$\gamma_{nc} = \frac{V^2}{R_c} - g\delta$$

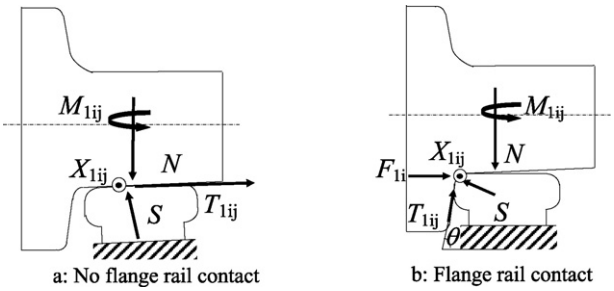

Fig. 3. The WR contact forces.

4. Safety and comfort

In tracks with a low radius of curvature, we have a flange rail contact. This contact leads to a lateral force that if it exceeds a certain limit, it can cause the derailment of the RV. Moreover, this kind of motion is usually accompanied by the creep of the wheel on the rail. This creeping generates the wear of the rail as well as of the wheel. It is generally accompanied by a high noise level.

4.1. The derailment force

When we have a flange rail contact, the y_{1i}^* variable of the vector $\mathbf{q}$ are constant and they present known values. By using the constraint equation $\dot{y}_{1i}^* = 0$ in the dynamic model (Eq. (11)), the Lagrange multiplier representing the lateral forces F_{1i} applied by each wheelset ($i = 1, 2$) on the rail can be calculated as follows:

$$F_{1i} = 2K_y y_1^* - (-1)^i 2K_y a\alpha_1^* + 2\chi C_{22}\alpha_{1i} \sum_i + (m + \hat{m})\gamma_{nc} - W\zeta(y_0 + y_{1i}^*) \tag{12}$$

In this case, the rail exerts two reacting forces on each wheel: the force S normal to the contact surface and the creep force T_{1ij} tangent to the contact surface.

The equilibrium forces (Fig. 3b) in the lateral direction yields

$$F_{1i} = S\sin\theta - T_{1ij}\cos\theta \tag{13}$$

The equilibrium forces (Fig. 3b) in the vertical direction yields:

$$N = S\cos\theta + T_{1ij}\sin\theta \tag{14}$$

The analysis of Eqs. (13) and (14) yields:

$$\frac{F_{1i}}{N} = \frac{\tan\theta - T_{1ij}/S}{1 + (T_{1ij}\tan\theta)/S} \tag{15}$$

The first term in Eq. (15) can be considered as a criterion of safety [7]. The maximum of safety is obtained when this term is minimal. The maximum of T_{1ij}/S corresponds to the friction coefficient μ. Therefore, at a given maximum contact angle, to avoid the derailment, we should have:

$$\frac{F}{N} < \frac{\tan\theta_{\max} - \mu}{1 + \mu\tan\theta_{\max}} \quad (F = \max(F_{1i})) \tag{16}$$

4.2. The creep forces

When a wheel rolls on the rail, relative slip can occur between the wheel and the rail at their contact. The slip generates a creep force at the wheel–rail interface in longitudinal (X_{1ij}) and lateral (T_{1ij}) directions and a torque (M_{1ij}). The creep forces are modeled based on the method proposed by Joly [2]. These elements are depicted in (Fig. 3a):

Table 2
The design parameters of the RV system.

The suspension and gyration parameters			
	$u = x$	$u = y$	$u = z$
ς_u (m)	0.58	0.4	0.58
Ω_u (m)	0.61	0.72	0.72
$\bar{\Omega}_u$ (m)	1.27	6.63	6.63
K_u (N/m)	3.15×10^7	3.96×10^6	2.1×10^6
$\bar{K}_u$ (N/m)	0.00	1.97×10^5	6.87×10^5

The geometric parameters			
e_0 (m)	0.75	d (m)	0.813
γ_e	0.1	$\bar{d}$ (m)	0.58
a (m)	1.04	l (m)	0.815
r_0 (m)	0.356	h (m)	0.305
$\bar{A}$ (m)	8.23	R_c (m)	280

The masses (Kg)		
$m + \hat{m}$	$\bar{M}$	M
1190	32 820	3072

$$X_{1ij} = (-1)^{j+1} C_{11} \frac{\gamma_e}{r_0} y^*_{1i} \sigma_i \tag{17}$$

$$T_{1ij} = C_{22} \alpha_{1i} \sum_i \tag{18}$$

$$M_{1ij} = C_{23} \alpha_{1i} \tag{19}$$

where the C_{ij} are the Kalker's coefficients ([2,8]).

The maximum of the creep resultant force is given by:

$$R = \max(R_{1ij}) = \max\left(\sqrt{X^2_{1ij} + T^2_{1ij}}\right) \tag{20}$$

5. Validation of the developed model

5.1. Solving algorithm

The obtained model is highly nonlinear. In order to determine these forces, F and R, we should have the system generalized coordinates. To achieve this goal, we developed an iterative algorithm, which solved the model in $\mathbf{q}$, based on the Broyden's method [9]. For an initial vector $\mathbf{q}$ ($\mathbf{q}_0 = 0$), this algorithm solves iteratively the dynamic model by minimizing the ration of the Euclidian norm of the increment to the Euclidian norm of the vector $\mathbf{q}$, solution of the model. This index should be less than a prefixed value. The values of F ($F = \max(F_{1i})$) and R are calculated using Eqs. (12) and (20).

5.2. Validation of the developed model

In this section, we will validate the developed model using results from the bibliography and numerical simulations using the software ADAMS. We have used the design parameters of a RV system given by He and McPhee [5] (Table 2). The RV traveling speed is $V = 13\ \mathrm{m\,s^{-1}}$.

The same design parameters are introduced in a virtual prototype. Fig. 4 shows the *erri_Wagon* model designed using ADAMS/Rail software. For this model, each spring is modeled to act in the three directions with different stiffness coefficients. By using ADAMS post processing, we can get the required simulation results.

With the same parameters, He and McPhee [5] have used the RGEM and RACES programs to generate automatically the governing equations and to solve them numerically. The software RACES was used to simulate the vehicle as it travels on a constant radius curve.

The use of these parameters (Table 2) in our algorithm and the simulation of the virtual prototype using ADAMS yield the results summarized in Table 3.

It is worth mentioning that the best validation of our model should be done using experimental results. However, these results are not found in the bibliography and the experiments required are expensive to perform. To build a comparison we have used as a reference the mean of the three results (Mcphee, ADAMS, and our analytical model). The error, relative to the mean of the three forces, is given by:

$$E_F = \frac{|\Delta F|}{F_m} = \frac{|F - F_m|}{F_m} \tag{21}$$

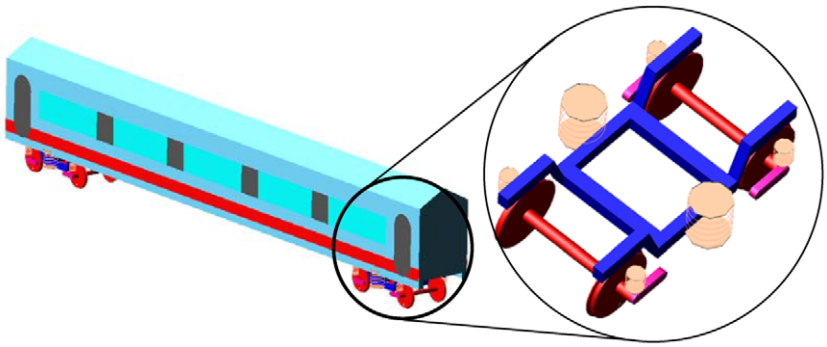

Fig. 4. The Erri_Wagon RV model (ADAMS).

Table 3
Results recapitulative.

	Forces (N)		Relative error (%)	
	F (N)	R (N)	E_F	E_R
Analytical model	3.51×10^4	1.28×10^4	2	3
ADAMS	3.35×10^4	1.36×10^4	2	3
He and McPhee	3.42×10^4	–	0	–

F is the force given by each method and F_m is the mean force given by the different methods.

We have not found a result concerning the creep force in [5]. From Table 3, one can note that the relative error of the derailment force and the creep force do not exceed 3%. Therefore, the obtained results are in agreement, which validates the developed model and the adopted hypotheses. This model has the advantages to be analytic and simple. Therefore, it can be easily used for the optimization of the RV design based on the safety and comfort criteria as well as the sensitivity of its performance to the design parameters fluctuations.

6. Conclusion

This work deals with the modeling of the rail vehicle behavior in short radius curves. Based on the symmetry of the vehicle and on the motion nature, we have shown that the study of the system behavior can be reduced to the quasi static study of its quarter. A quasi static model was developed in a closed form. This model is able to describe the dynamic behavior of a rail vehicles system. By using this model, the safety and the comfort criteria were expressed as functions of the derailment and the creep forces. The developed model is validated by bibliographic results and using the software ADAMS.

The developed model can be easily used for the optimization design of the rail vehicle and the sensitivity analyses of its performances.

References

[1] K. Dang Van, Modelling of damage induced by contacts between solids, C. R. Mécanique 336 (2008) 91–101.
[2] R. Joly, Circulation d'un véhicule ferroviaire en courbe de faible rayon, Journal Rail International (1988) 31–42.
[3] I.Y. Shevtsov, V.L. Markine, C. Esveld, Optimal design of wheel profile for railway vehicles, Wear 258 (2005) 1022–1030.
[4] M. Majka, M. Hartnett, Effects of speed, load and damping on the dynamic response of railway bridges and vehicles, Computers and Structures 86 (2008) 556–572.
[5] Y. He, J. McPhee, Optimization of curving of rail vehicles, Vehicle System Dynamics 43 (2005) 895–923.
[6] H. Rjeb, Z. Affi, H. Bettaieb, Optimization of the design variables of rail vehicles system in rectilinear motion, in: The Second International Congress Design and Modeling of Mechanical Systems, CMSM'2007, 2007.
[7] J. Elkins, H. Wu, Angle of attack and distance based criteria for flange climb derailment, Vehicle System Dynamics Supplement 33 (1999) 293–305.
[8] S. Datoussaid, Optimisation du comportement dynamique et cinématique des systèmes multicorps a structure cinématique complexe, Ph.D. these, Faculté polytechnique de Mons, Belgique, 1998.

[9] J. Nocedal, S.J. Wright, Numerical Optimization, Springer-Verlag, New York, Inc, ISBN 0-387-98793-2, 1999.
[10] Y. Li, Sh. Qiang, H. Liaoa, Y.L. Xu, Dynamics of wind–rail vehicle–bridge systems, Journal of Wind Engineering and Industrial Aerodynamics 93 (2005) 483–507.
[11] Y.-C. Cheng, et al., Modeling and nonlinear hunting stability analysis of high-speed railway vehicle moving on curved tracks, Journal of Sound and Vibration 324 (2009) 139–160.